Jurnal CoreIT, Vol 9, No 1, June 2023
ISSN 2460-738X (Print)
ISSN 2599-3321 (Online)

Identification of an Individual's Iris Using Euclidean and Mahalanobis Diagrams

Novan Wijaya[1*], Hafiz Irsyad[2], Akhsani Taqwiym[3]
[1*]Dept. of Informatics Management, Universitas Multi Data Palembang, Indonesia
[2]Dept. of Informatics, Universitas Multi Data Palembang, Indonesia
[3]Dept. of Information System, Universitas Multi Data Palembang, Indonesia
[1*]novan.wijaya@mdp.ac.id, [2]hafizirsyad@mdp.ac.id, [3]akhsani.taqwiym@mdp.ac.id

Abstract. The purpose of this study is to compare Euclidean and Mahalanobis geometry as a means of identifying a person using their iris. Iris is the only biometric that is truly unique and is extremely difficult to perform, making it the single most important consideration in the improvement of system security. To obtain the desired results, namely preprocessing and feature extraction, various methods will be used in image processing. Methods like the Gaussian filter, the operator sobel, and thresholding will be used in the pengolahan. Utilize the United Moment Invariant method to extend the circle (UMI). For projects that use the method of comparing the strengths of FAR and GAR, a smaller FAR was obtained for the eulidean to mahalanobis ratio. Additionally, value distance mahalanobis is smaller compared to FAR for GAR penetration.

Keywords: Gaussian Filter, Iris, Sobel Operator, United Moment Invariat

Received October 2022 / **Revised** January 2023 / **Accepted** June 2023

INTRODUCTION

The iris of the eye is a unique pattern in the human body that can be utilized as an identification tool in biometric systems. Iris has various features, like being stable, having a diversified physical structure, and not relying on hereditary traits. As a result, the iris can be used as a personal identity, and a human iris recognition system is now being developed. Biometric systems, in addition to being able to be used as a security medium, have also been developed for identification in the health sector, as demonstrated by the study [1] "Classification of Heart Abnormalities Through Iris Image Using Fuzzy C-Means as Iris Feature Extractor and Classification Using Support Vector Machine." The study's findings revealed that 75% of the time, identification was successful. An identification success rate of 90% was found in the study "Pre-Diagnosis of Kidney Disorders Through Iris Image Using Raspberry PI With Convolutional Neural Network (CNN) Method" [2].

The researchers used a combination of approaches in their investigation from many studies that were conducted. For example, [3], which combines the Daubechies wavelet approach, 2D wavelet transform, and K-Nearest Neighbor. [4] is a combination of the canny operator, the circle hough transformation, and the Euclidean distance method. [5] combines the operator approaches Canny, GLCM, and SVM. This study is significant since it is the first to combine the Gaussian Filter as picture pre-processing, edge detection with the Sobel operator approach, United Moment Invariants (UMI) for iris image feature extraction, and Euclidean and Mahalanobis distance algorithms for iris recognition.

LITERATURE REVIEW

A. Preprocess

Preprocessing seeks to improve the quality of the iris picture in order to make further processing easier. The database utilized to collect iris images was the CASIA v4.0 database [6]. as well as many preprocessing algorithms, such as the Gaussian Filter [7]. The goal of this procedure is to reduce noise from the iris.

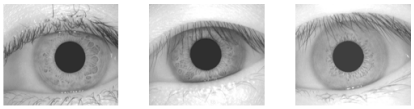

Figure 1. Iris eye casia v4.0

DOI: 10.24014/coreit.v9i1.18681

B. Thresholding

The thresholding method employed is double thresholding. The floating process employs two threshold values, H (High threshold) and L (Low threshold). If a point's value is greater than H, it will be accepted immediately. In contrast, if a point's value is less than L, it is instantly eliminated. If a point's value is between H and L, it will be approved if it is close to a pixel with a strong reaction [8].

C. Segmentation of the Iris

Image segmentation is the process of distinguishing one object in an image from another [9]. Edge detection using the Sobel operator approach and iris localization using the Bipolar Transformation method are used in the segmentation procedure [10].

D. Extraction of Iris Features

The goal of feature extraction is to retrieve the most important aspects of an image. The iris of the eye is being extracted using the unired moment invariants (UMI) approach [11].

E. Distance in Euclidean terms

The most often used metric for calculating the similarity of two vectors is Euclidean distance. The difference in pixel values between the two test image feature vectors (query) and the training image feature vector is defined as the Euclidean distance [12].

$$\mathrm{ED}(x, y) = \sqrt{\sum_{i=1}^{n}(x_i - y_i)^2} \qquad (1)$$

Where :

ED : Euclidean distance

x_i : Query image

y_i : Database image

n : Number of vectors x and y.

F. Distance of Mahalanobis

The Mahalanobis distance is a statistical approach for grouping data based on a distance. The Mahalanobis distance was utilized in this study to compare two feature matrices of an iris that had undergone a feature extraction method [13].

$$\mathrm{MD}(x, y) = \sqrt{(x - y)^T S^{-1}(x - y)} \qquad (2)$$

Where :

x : Query picture

y : Database image

$(x-y)^T$: Matrix transpose

$S^{-1}(x-y)$: inverse covariance matrix

A threshold is utilized to determine whether the query image is accepted or refused [14]. If the ED and MD distances are less than the set threshold, the system will accept the query image; otherwise, if the ED and MD distances are greater than the threshold, the system will reject the query image.

METHODS

A. Analysis of Preprocessing

Preprocessing improves iris recognition accuracy based on iris pattern images [15]. The picture preprocessing itself tries to improve the quality of the iris image. The following picture preprocessing techniques were used in the current study:

Smoothing of Images

The image is smoothed for the first time with a Gaussian filter. Gaussian filtering is used to eliminate noise from the ocular image, resulting in a better image.

Detection of the Edge

Following the picture refinement procedure, the next step is to locate the iris image's contour. The Sobel operator is used to find the edge [16]. The Sobel operator employs a pair of 3x3 convolution matrices, one of which predicts the gradient value in the x direction and the other in the y direction.

Sharpening of the Edges

The goal of this phase is to sharpen the edges obtained during the previous operation. In this stage, we will locate the image's local maximum of gradient magnitudes.

B. Separation of Feature Extraction

Following the completion of the preprocessing phase, the next step is feature separation. The feature separation process is made up of the following steps:

Identification of the Iris

The Hough transform method is used in the localization iris process. Using the edges of the item, we can use the Hough transform to determine the shape of other objects in the image.

Normalization of the Iris

The normalization procedure seeks to acquire the iris area within a specific dimension to aid in feature extraction calculations. Image geometry operations, such as rotation and translation, are used in the normalization process.

C. Extraction of Iris Features

The UMI (United Moment Invariant) approach is used to extract the features of the iris image. United Moment Invariant (UMI) is a pattern recognition feature extraction method. [11]invented this technique. This method is thought to be capable of compensating for the inadequacies of the prior moment invariant method. The benefit of this strategy is that it may be used in discrete settings as well as based on observations, areas, and boundaries. The extraction technique generates eight feature vectors using the United Moment Invariant (UMI). The UMI process results are saved in a database.

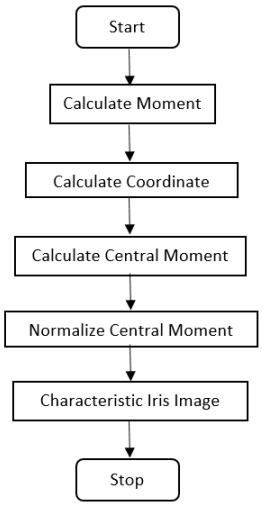

Figure 2. Flowchart of the UMI process

The initial stage in the iris feature extraction process is to enter an image of the eye's iris, after which the image goes through a preprocessing process, followed by the UMI process, and the results of the UMI process are saved in the database. The UMI process will include calculating the moment, calculating the center point, calculating the central moment, calculating the normalized central moment, calculating the moment invariant, and finally calculating eight formulas from UMI to obtain the characteristics of the iris image figure 2 depicts this.

Figure 3 depicts the iris recognition procedure, which will begin after the iris image is entered. Then, using the UMI approach, extract the features, figure 2 depicts the feature extraction procedure. Following that, the Euclidean and Mahalanobis distances will be calculated, which will match the feature vector of the newly entered iris image with the feature vector of the picture databases. After getting the Euclidean and Mahalanobis distance values and comparing the distance values with a threshold value, the process of finding the threshold value is a process of determining the optimal threshold value to give the greatest system performance.

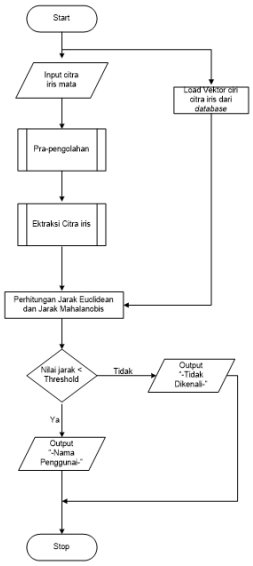

Figure 3. Flowchart for identifying iris images

D. Analysis of the Iris Test

The FAR and GAR values will be calculated based on the results of the identification to assess the capability of the iris identification system. Equation 3 shows the equation for calculating the FAR value, and Equation 4 shows the equation for calculating the GAR value.

$$FAR = \frac{Number\ of\ False\ Author\ Matches}{Number\ of\ False\ Data\ Matches} x100\% \quad (3)$$

$$GAR = \frac{Number\ of\ Correct\ Matches}{Number\ of\ Correct\ Data\ Matches} x\ 100\% \quad (4)$$

RESULTS AND DISCUSSIONS

A. Preprocessing Test Results

Figure 4 depicts the outcome of the preprocessing procedure. The pre-processing processes are performed the first time the user inputs the iris image by selecting 'Open Image' from the file menu. The user then selects the 'Image Refinement,' 'Edge Detection,' 'Edge Sharpening,' and 'Thresholding' options. The pre-processing step is used to obtain the iris image's edges.

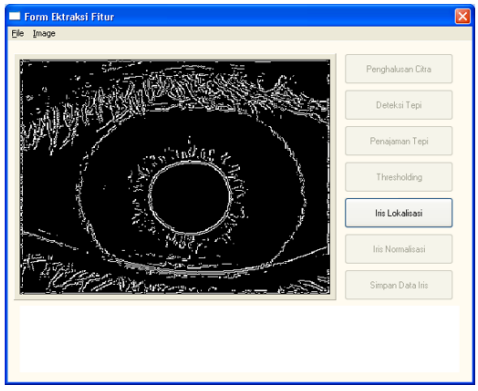

Figure 4. Preprocessing Examination

B. Test Results for Feature Extraction

Following the completion of the pre-processing phase, the next step is feature separation. To begin the feature separation process, press the 'Localization Iris' button, followed by the 'Normalized Iris' button. The image below depicts the results of the feature separation test.

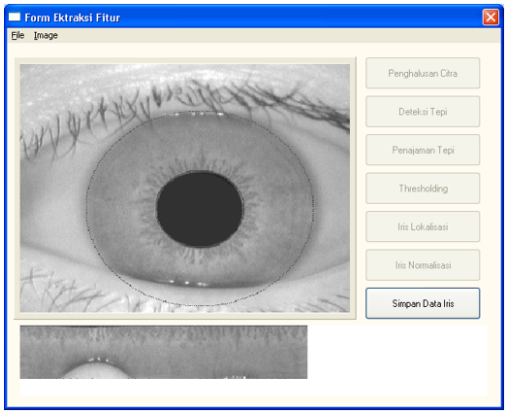

Figure 5. Feature Extraction Examination

According to Figure 5, the feature extraction procedure is working properly. The feature separation technique seeks to provide an image of the eye's iris that has been separated from other elements of the eye, such as the pupil and sclera.

C. Test Results for Iris Identification

In Figures 6 and 7, the user initially searches for the iris picture file to be detected before pressing the 'Detect' button. The system performs the full pre-processing procedure until the feature separation is completed and a comparison is done with the data in the database. If the owner of the iris data is identified, the system will display the owner's name as well as the results of the Euclidean and Mahalanobis distance calculations. If the data is not recognized, the system will display the name "-Unrecognized-" as the result.

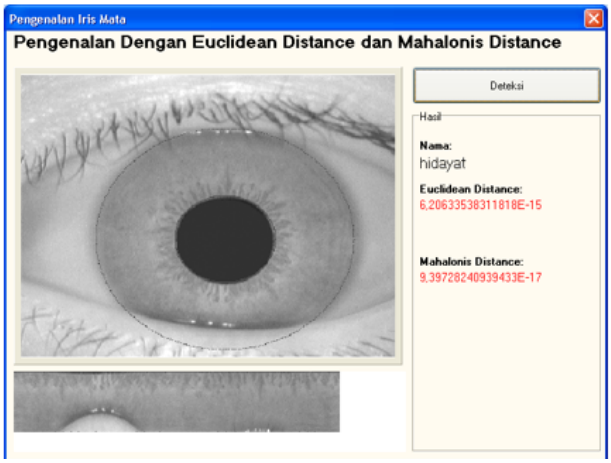

Figure 6. Succesful Identification

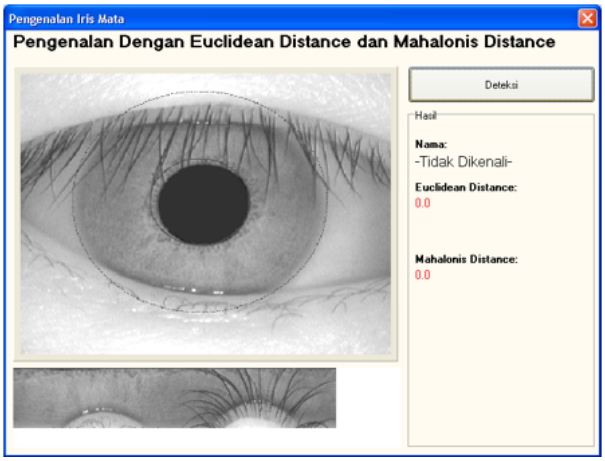

Figure 7. Unsuccesful Identification

Table 1. shows the results of the query image test with the database picture using a 0.1 Euclidean distance threshold.

Image Testing (.bmp)	Results		Conclusion
	Name	Euclidean Distance	
005-1	-	0,828498	Not Recognized
005-2	Iris 3	0,066085	Recognized
005-3	Iris 1	0,078583	Recognized
006-1	-	0,110834	Recognized
006-2	Iris 4	0,002792	Recognized
006-3	-	0,147037	Not Recognized
007-1	Iris 4	0,007919	Recognized
007-2	Iris 3	0,022680	Recognized
007-3	Iris 4	0,073230	Recognized
008-1	-	7,875757	Not Recognized
008-2	-	0,477270	Not Recognized
008-3	Iris 1	0,090199	Recognized
009-1	Iris 2	0,076423	Recognized
009-2	Iris 3	0,012322	Recognized
009-3	Iris 3	0,028370	Recognized
010-1	Iris 4	0,023718	Recognized
010-2	Iris 4	0,035442	Recognized
010-3	Iris 4	0,035908	Recognized
011-1	-	0,127160	Not Recognized
011-2	Iris 1	0,070921	Recognized
011-3	Iris 3	0,014564	Recognized
012-1	Iris 4	0,076107	Recognized
012-2	-	0,127932	Not Recognized
012-3	-	0,485577	Not Recognized
013-1	-	0,244573	Not Recognized
013-2	-	0,419562	Not Recognized
013-3	-	0,362595	Not Recognized
014-1	-	0,137812	Not Recognized
014-2	Iris 4	0,091368	Recognized
014-3	-	28,57775	Not Recognized
015-1	-	0,201815	Not Recognized
015-2	-	0,110140	Not Recognized
015-3	-	0,270308	Not Recognized
016-1	-	0,774378	Not Recognized
016-2	Iris 3	0,006086	Recognized
016-3	Iris 3	0,010145	Recognized
017-1	-	0,100125	Not Recognized
017-2	-	0,300499	Not Recognized
017-3	Iris 1	0,078044	Recognized
018-1	-	0,232630	Not Recognized
018-2	-	0,338435	Not Recognized
018-3	-	0,408332	Not Recognized
019-1	Iris 4	0,043903	Recognized

019-2	Iris 4	0,034114	Recognized
019-3	Iris 4	0,034093	Recognized
020-1	-	0,262187	Not Recognized
020-2	Iris 1	0,071097	Recognized
020-3	-	14,62669	Not Recognized
021-1	Iris 1	0,047969	Recognized
021-2	Iris 1	0,055315	Recognized
021-3	Iris 1	0,040792	Recognized
022-1	Iris 4	0,071446	Recognized
022-2	Iris 4	0,045617	Recognized
022-3	-	0,104297	Not Recognized
023-1	Iris 3	0,008911	Recognized
023-2	Iris 3	0,032884	Recognized
023-3	Iris 3	0,011267	Recognized
024-1	-	0,115565	Not Recognized
024-2	Iris 4	0,069825	Recognized
024-3	Iris 1	0,067485	Recognized
025-1	-	0,239109	Not Recognized
025-2	-	0,318764	Not Recognized
025-3	-	0,203209	Not Recognized
026-1	Iris 4	0,072847	Recognized
026-2	Iris 4	0,050185	Recognized
026-3	-	0,134366	Not Recognized
027-1	Iris 3	0,030802	Recognized
027-2	Iris 3	0,017628	Recognized
027-3	Iris 3	0,005321	Recognized
028-1	Iris 4	0,056943	Recognized
028-2	Iris 3	0,005566	Recognized
028-3	Iris 3	0,004098	Recognized
029-1	-	0,206838	Not Recognized
029-2	Iris 4	0,074610	Recognized
029-3	-	1,201252	Not Recognized
030-1	Iris 3	0,013452	Recognized
030-2	Iris 4	0,083326	Recognized
030-3	Iris 4	0,083326	Recognized
031-1	Iris 3	0,003735	Recognized
031-2	Iris 3	0,046628	Recognized
031-3	Iris 3	0,028033	Recognized
032-1	-	0,134538	Not Recognized
032-2	Iris 3	0,011351	Recognized
032-3	-	0,154224	Not Recognized
033-1	-	0,328420	Not Recognized
033-2	-	0,461389	Not Recognized
033-3	Iris 3	0,016570	Recognized
034-1	-	0,109097	Not Recognized
034-2	Iris 4	0,071436	Recognized
034-3	-	0,151014	Not Recognized

035-1	Iris 4	0,054859	Recognized
035-2	Iris 3	0,034153	Recognized
035-3	Iris 3	0,006024	Recognized
036-1	Iris 1	0,067224	Recognized
036-2	-	6,211768	Not Recognized
036-3	Iris 1	0,083861	Recognized
037-1	Iris 4	0,051899	Recognized
037-2	Iris 4	0,051918	Recognized
037-3	Iris 4	0,045401	Recognized
038-1	Iris 4	0,046118	Recognized
038-2	-	0,119646	Not Recognized
038-3	Iris 4	0,098166	Recognized
040-1	-	0,239074	Not Recognized
040-2	Iris 1	0,045772	Recognized
040-3	Iris 1	0,043251	Recognized
041-1	Iris 4	0,041531	Recognized
041-2	Iris 4	0,067304	Recognized
041-3	-	0,391507	Not Recognized
042-1	Iris 1	0,084082	Recognized
042-2	Iris 1	0,092071	Recognized
042-3	Iris 1	0,084388	Recognized
043-1	Iris 1	0,084470	Recognized
043-2	Iris 3	0,013416	Recognized
043-3	Iris 4	0,035522	Recognized
044-1	-	0,246229	Not Recognized
044-2	-	2,262075	Not Recognized
044-3	-	168,4379	Not Recognized
045-1	Iris 4	0,049372	Recognized
045-2	Iris 2	0,021906	Recognized
045-3	Iris 4	0,099214	Recognized
046-1	-	0,164155	Not Recognized
046-2	-	0,231146	Not Recognized
046-3	-	0,166243	Not Recognized
047-1	Iris 2	0,048690	Recognized
047-2	-	0,136777	Not Recognized
047-3	Iris 2	0,050223	Recognized
048-1	Iris 2	0,058297	Recognized
048-2	Iris 1	0,083718	Recognized
048-3	Iris 2	0,018445	Recognized
049-1	Iris 2	0,055372	Recognized
049-2	Iris 1	0,090004	Recognized
049-3	Iris 1	0,090007	Recognized
050-1	Iris 4	0,089660	Recognized
050-2	Iris 4	0,042702	Recognized
050-3	Iris 4	0,052464	Recognized

Table 2. shows the identification of iris data in the system using 12 samples of data from 4 people using Euclidean Distance.

Image Testing (.bmp)	Results		Conclusion
	Name	Euclidean Distance	
001-1	Iris 1	0,083724	Recognized
001-2	Iris 1	0,084530	Recognized
001-3	Iris 1	0,095496	Recognized
002-1	Iris 2	3,800791	Recognized
002-2	Iris 2	0,002133	Recognized
002-3	-	3,797409	Not Recognized
003-1	Iris 3	4,648375	Recognized
003-2	-	0,102312	Not Recognized
003-3	Iris 3	0,051038	Recognized
004-1	Iris 4	5,721689	Recognized
004-2	Iris 4	0,089560	Recognized
004-3	Iris 4	0,032057	Recognized

Based on the results of the tests, the Recognized and Not Recognized irises with a local threshold are determined. This test data is obtained from unregistered data samples for iris data that can be recognized as many as 87 times and cannot be recognized as many as 48 times. Meanwhile, 10 iris data with test data acquired from reference data are recognized, while 2 are not.

$$FAR = \frac{87}{135} x100\% = 64.44\%$$

$$GAR = \frac{10}{12} x100\% = 83{,}33\%$$

Table 3. shows the results of the query image test with the database picture using a 0.1 Mahalanobis distance threshold.

Image Testing (.bmp)	Results		Conclusion
	Name	Mahalanobis Distance	
005-1	Iris 3	0,002892545	Recognized
005-2	Iris 3	0,003150653	Recognized
005-3	Iris 2	0,012458579	Recognized
006-1	Iris 4	0,016093011	Recognized
006-2	Iris 4	0,000146809	Recognized
006-3	Iris 4	0,021155140	Recognized
007-1	Iris 4	0,001519273	Recognized
007-2	Iris 2	0,003137114	Recognized
007-3	Iris 4	0,010830984	Recognized
008-1	Iris 4	0,001354901	Recognized
008-2	Iris 1	0,028243437	Recognized
008-3	Iris 1	0,027856805	Recognized
009-1	Iris 2	0,003171102	Recognized
009-2	Iris 3	0,000284150	Recognized
009-3	Iris 2	0,003156357	Recognized
010-1	Iris 4	0,013477994	Recognized
010-2	Iris 4	0,013464421	Recognized

010-3	Iris 4	0,013467068	Recognized
011-1	Iris 1	0,027423821	Recognized
011-2	Iris 1	0,027240112	Recognized
011-3	Iris 3	0,003152841	Recognized
012-1	Iris 4	0,011098633	Recognized
012-2	Iris 4	0,020332400	Recognized
012-3	Iris 4	0,075901618	Recognized
013-1	Iris 1	0,027663179	Recognized
013-2	Iris 4	0065433880	Recognized
013-3	Iris 4	0,056792661	Recognized
014-1	Iris 4	0,021292018	Recognized
014-2	Iris 4	0,013502568	Recognized
014-3	Iris 3	0,000461540	Recognized
015-1	Iris 4	0,325363909	Recognized
015-2	Iris 4	0,016574333	Recognized
015-3	Iris 4	0,042614306	Recognized
016-1	Iris 3	0,002906500	Recognized
016-2	Iris 3	0,003130001	Recognized
016-3	Iris 3	0,003130323	Recognized
017-1	Iris 4	0,014840241	Recognized
017-2	Iris 4	0,047722750	Recognized
017-3	Iris 1	0,078044469	Recognized
018-1	Iris 4	0,035920398	Recognized
018-2	Iris 4	0,052913228	Recognized
018-3	Iris 4	0,063500034	Recognized
019-1	Iris 4	0,004389013	Recognized
019-2	Iris 4	0,000334384	Recognized
019-3	Iris 4	0,000454490	Recognized
020-1	Iris 1	0,027702424	Recognized
020-2	Iris 1	0,027241303	Recognized
020-3	Iris 1	0,000849085	Recognized
021-1	Iris 1	0,027156569	Recognized
021-2	Iris 3	0,003146092	Recognized
021-3	Iris 2	0,012457809	Recognized
022-1	Iris 4	0,010738095	Recognized
022-2	Iris 4	0,005656737	Recognized
022-3	Iris 4	0,016502743	Recognized
023-1	Iris 3	0,003129956	Recognized
023-2	Iris 3	0,003140028	Recognized
023-3	Iris 3	0,003134486	Recognized
024-1	Iris 1	0,027349772	Recognized
024-2	Iris 4	0,010897989	Recognized
024-3	Iris 1	0,027219857	Recognized
025-1	Iris 1	0,027646783	Recognized
025-2	Iris 4	0,047658367	Recognized
025-3	Iris 1	0,027559376	Recognized
026-1	Iris 4	0,012788330	Recognized

026-2	Iris 4	0,006998882	Recognized
026-3	Iris 4	0,019341113	Recognized
027-1	Iris 3	0,003139228	Recognized
027-2	Iris 3	0,003127414	Recognized
027-3	Iris 3	0,003130662	Recognized
028-1	Iris 4	0,007116900	Recognized
028-2	Iris 3	0,003130877	Recognized
028-3	Iris 3	0,003131156	Recognized
029-1	Iris 4	0,033277389	Recognized
029-2	Iris 4	0,010967581	Recognized
029-3	Iris 3	0,002765772	Recognized
030-1	Iris 3	0,003128565	Recognized
030-2	Iris 4	0,012273250	Recognized
030-3	Iris 3	0,003150736	Recognized
031-1	Iris 3	0,003132493	Recognized
031-2	Iris 3	0,003142947	Recognized
031-3	Iris 3	0,003125175	Recognized
032-1	Iris 4	0,019581041	Recognized
032-2	Iris 3	0,003130009	Recognized
032-3	Iris 4	0,022031713	Recognized
033-1	-	0,050724053	Recognized
033-2	Iris 4	0,068855491	Recognized
033-3	Iris 3	0,003128096	Recognized
034-1	Iris 4	0,017712109	Recognized
034-2	Iris 4	0,010369749	Recognized
034-3	Iris 4	0,024576264	Recognized
035-1	Iris 4	0,007139048	Recognized
035-2	Iris 3	0,003123426	Recognized
035-3	Iris 3	0,003130991	Recognized
036-1	Iris 1	0,027243246	Recognized
036-2	Iris 3	0,001550413	Recognized
036-3	Iris 1	0,027279858	Recognized
037-1	Iris 4	0,006560831	Recognized
037-2	Iris 4	0,007029501	Recognized
037-3	Iris 4	0,005997529	Recognized
038-1	Iris 1	0,027646250	Recognized
038-2	Iris 1	0,027153999	Recognized
038-3	Iris 4	0,098166360	Recognized
040-1	Iris 1	0,027646250	Recognized
040-2	Iris 1	0,027153999	Recognized
040-3	Iris 2	0,012450382	Recognized
041-1	Iris 4	0,003869876	Recognized
041-2	Iris 4	0,008788944	Recognized
041-3	Iris 4	0,060669454	Recognized
042-1	Iris 1	0,027118621	Recognized
042-2	Iris 1	0,027194290	Recognized
042-3	Iris 1	0,027123622	Recognized

043-1	Iris 1	0,027126611	Recognized
043-2	Iris 3	0,003129596	Recognized
043-3	Iris 4	0,001586445	Recognized
044-1	Iris 4	0,038283052	Recognized
044-2	Iris 3	0,002327886	Recognized
044-3	Iris 3	9,484623026	Recognized
045-1	Iris 4	0,004853448	Recognized
045-2	Iris 3	0,003141347	Recognized
045-3	Iris 4	0,014648463	Recognized
046-1	Iris 4	0,025982886	Recognized
046-2	Iris 4	0,035673625	Recognized
046-3	Iris 4	0,027394432	Recognized
047-1	Iris 3	0,003147032	Recognized
047-2	Iris 1	0,027359988	Recognized
047-3	Iris 3	0,003147926	Recognized
048-1	Iris 3	0,003149943	Recognized
048-2	Iris 1	0,027105030	Recognized
048-3	Iris 3	0,003140057	Recognized
049-1	Iris 3	0,003148571	Recognized
049-2	Iris 1	0,027174358	Recognized
049-3	Iris 1	0,027174296	Recognized
050-1	Iris 4	0,014374754	Recognized
050-2	Iris 4	0,004905637	Recognized
050-3	Iris 4	0,007478313	Recognized

Tabel 4. Shown the identification of iris data in the system using 12 samples of data from 4 peaple using mahalanobis distance.

Citra Testing (.bmp)	**Results**		**Conclusion**
	Name	**Mahalanobis Distance**	
001-1	Iris 1	0,041589672	Recognized
001-2	Iris 1	0,041637605	Recognized
001-3	Iris 1	0,041765041	Recognized
002-1	Iris 2	0,012386470	Recognized
002-2	Iris 2	0,012384674	Recognized
002-3	Iris 2	0,008465065	Recognized
003-1	Iris 3	0,003131655	Recognized
003-2	Iris 3	0,015082571	Recognized
003-3	Iris 3	0,010300095	Recognized
004-1	Iris 4	1,925032144	Recognized
004-2	Iris 4	0,012914244	Recognized
004-3	Iris 4	0,004644225	Recognized

Based on the results of the tests, the Recognized and Not Recognized irises with a local threshold are determined. This test data is obtained from unregistered data samples for iris data that can be Recognized as much as 135 and Not Recognized as 0. Meanwhile, 12 of the iris data with test data acquired from reference data are Recognized and 0 are Not Recognized.

$$FAR = \frac{135}{135} x100\% = 100\%$$

$$GAR = \frac{12}{12} x100\% = 100\%$$

CONCLUSION

The FAR accuracy rate for iris identification using the Euclidean distance is 64.44 percent, but it is 100 percent utilizing the Mahalanobis FAR distance. The success ratio, or GAR, obtained from the system's identification results using the Euclidean distance is 83.33 percent, while using the Mahalanobis distance is 100 percent. According to the GAR value, the Mahalanobis distance has a better percentage of successful iris recognition than the Euclidean distance. The greater the GAR value, the higher the system identification success rate in recognizing the same iris.

REFERENCES

[1] D. C. rini Novitasari, M. F. Rozi, and R. Veriani, "Klasifikasi Kelainan Pada Jantung Melalui Citra Iris Mata Menggunakan Fuzzy C-Means Sebagai Pengambil Fitur Iris Dan Klasifikasi Menggunakan Support Vector Machine," *INTEGER J. Inf. Technol.*, vol. 4, no. 1, pp. 1–10, 2019, doi: 10.31284/j.integer.2019.v4i1.489.

[2] I. Agustian, F. Hadi, and M. K. A. Rosa, "Pre-Diagnosis Gangguan Ginjal Melalui Citra Iris Mata Menggunakan Raspberry PI Dengan Metode Convolutional Neural Network (CNN)," *J. Amplif. J. Ilm. Bid. Tek. Elektro Dan Komput.*, vol. 9, no. 1, pp. 16–25, 2019, doi: 10.33369/jamplifier.v9i1.15396.

[3] F. E. Alfian, I. G. P. S. Wijaya, and F. Bimantoro, "Identifikasi Iris Mata Menggunakan Metode Wavelet Daubechies dan K-Nearest Neighbor," *J. Teknol. Informasi, Komputer, dan Apl. (JTIKA)*, vol. 2, no. 1, pp. 1–10, 2020, doi: 10.29303/jtika.v2i1.76.

[4] K. Telaumbanua, P. Sirait, A. Rohana, and B. Gea, "Sistem Pengenalan Iris Mata Menggunakan Metode Wavelet Packets Decomposition dan Euclidean Distance," *J. SIFO Mikroskil*, vol. 20, no. 2, pp. 105–116, 2019, [Online]. Available: https://www.mikroskil.ac.id/ejurnal/index.php/jsm/article/view/668.

[5] I. A. Qasmieh, H. Alquran, and A. M. Alqud, "Occluded iris classification and segmentation using selfcustomized artificial intelligence models and iterative randomized Hough transform," *Int. J. Electr. Comput. Eng.*, vol. 11, no. 5, pp. 4037–4049, 2021, doi: 10.11591/ijece.v11i5.

[6] M. Arsalan, R. A. Naqvi, D. S. Kim, P. H. Nguyen, M. Owais, and ang R. Park, "IrisDenseNet: Robust Iris Segmentation Using Densely Connected Fully Convolutional Networks in the Images by Visible Light and Near-Infrared Light Camera Sensors," *Sensors*, vol. 18, no. 5, p. 1501, 2018, doi: 10.3390/s18051501.

[7] H. A. D. Rani, "Perbandingan Metode Filtering Untuk Peningkatan Kualitas Citra Iris Mata Berbasis Image Processing," *JOINED J. INFORMATICS Educ.*, vol. 1, no. 1, pp. 10–16, 2018, doi: 10.31331/joined.v1i1.622.

[8] N. Wijaya, H. Irsyad, and A. Taqwiym, "DESIGN VERIFICATION USING PALMPRINT," *TEKNOMATIKA*, vol. 07, no. 02, pp. 36–46, 2017.

[9] A. F. Amalia and H. Saputro, "Analisis deteksi iris mata menggunakan metode deteksi tepi sobel," *Sci. TECH J. Ilm. Ilmu Pengetah. dan Teknol.*, vol. 4, no. 1, pp. 41–48, 2018.

[10] K. Fitria and L. Hakim, "Segmentasi Region Of Interest (ROI) Garis Telapak Tangan Menggunakan Deteksi Tepi Sobel," *Explor. IT! J. Keilmuan dan Apl. Tek. Inform.*, vol. 11, no. 1, pp. 29–40, 2019, doi: 10.35891/explorit.v11i1.1666.

[11] B. O. Muhammed and S. M. Shamsuddin, "A multimodal biometric system using global features for identical twins identification," *J. Comput. Sci.*, vol. 14, no. 1, pp. 92–107, 2018, doi: 10.3844/jcssp.2018.92.107.

[12] Y. Miftahuddin, S. Umaroh, and F. R. Karim, "Perbandingan Metode Perhitungan Jarak Euclidean, Haversine, Dan Manhattan Dalam Penentuan Posisi Karyawan," *J. Tekno Insentif*, vol. 14, no. 2, pp. 69–77, 2020, doi: 10.36787/jti.v14i2.270.

[13] M. Azizah, A. Hidayatno, and Y. Christyono, "APLIKASI PENGENAL PENGUCAP BERBASIS IDENTIFIKASI SUARA DENGAN EKSTRAKSI CIRI MEL-FREQUENCY CEPSTRUM COEFFICIENTS (MFCC) DAN KUANTISASI VEKTOR Mega Tiara Nur Azizah *) , Achmad Hidayatno , and Yuli Christyono Abstrak Pendahuluan Metode," *Transient*, vol. 6, no. 4, pp. 639–643, 2017.

[14] A. K. Khairuzzaman and S. Chaudhury, "Multilevel thresholding using grey wolf optimizer for image segmentation," *Expert Syst. Appl.*, 2017, doi: 10.1016/j.eswa.2017.04.029.

[15] W. Zhou, X. Ma, and Y. Zhang, “Research on image preprocessing algorithm and deep learning of iris recognition,” *J. Phys. Conf. Ser.*, vol. 1621, no. 1, p. 012008, 2020, doi: 10.1088/1742-6596/1621/1/012008.

[16] K. Wardani, A. Kurniawan, and E. Mulyana, “ROI Based Post Image Quality Assessment Technique on Multiple Localized Filtering Method on Kinect Sensor,” in *In 2018 12th International Conference on Telecommunication Systems, Services, and Applications (TSSA)*, 2018, pp. 1–4, doi: 10.1109/TSSA.2018.8708810.